



HAL
open science

Diffraction by gratings: from C-method to Stochastic C-method

Jean Chandezon, Gérard Granet

► **To cite this version:**

Jean Chandezon, Gérard Granet. Diffraction by gratings: from C-method to Stochastic C-method. Journal of the Optical Society of America. A Optics, Image Science, and Vision, inPress, 10.1364/ao.XX.XXXXXX . hal-04642756

HAL Id: hal-04642756

<https://hal.science/hal-04642756v1>

Submitted on 10 Jul 2024

HAL is a multi-disciplinary open access archive for the deposit and dissemination of scientific research documents, whether they are published or not. The documents may come from teaching and research institutions in France or abroad, or from public or private research centers.

L'archive ouverte pluridisciplinaire **HAL**, est destinée au dépôt et à la diffusion de documents scientifiques de niveau recherche, publiés ou non, émanant des établissements d'enseignement et de recherche français ou étrangers, des laboratoires publics ou privés.

Diffraction by gratings: from C-method to Stochastic C-method

JEAN CHANDEZON^{1*} AND GÉRARD GRANET^{2,*}

¹Jean Chandezon, retired, former professor at Université Clermont Auvergne, 31 avenue du docteur Louis Presle, F63960 Veyre-Monton

²Université Clermont Auvergne, Clermont Auvergne INP,CNRS, Institut Pascal, F-63000 Clermont-Ferrand,France

^{1*}jean.chandezon@uca.fr

^{2*}gerard.granet@uca.fr

Compiled July 10, 2024

The Chandezon, or C-method, is an efficient and versatile numerical method for modeling diffraction problems involving smooth surface relief gratings. For some grating profiles, the C-method is limited when the height-to-period ratio exceeds a factor of 3. This is due to the formation of ill-conditioned matrices for inversion. Here, the Stochastic C-method (SCM) is introduced as a solution which leverages stochastic differential equations to overcome these numerical difficulties. The SCM is developed by altering the physical model of the grating profile function to include an additive Brownian noise component. The inclusion of noise, dramatically expands the applicability of the C-method and enriches the physical model. Numerical experiments show that the SCM achieves a precision on the order of 10^{-5} for diffracted/transmitted amplitudes on sinusoidal profiles with height-to-period ratios as high as 72. These results are in agreement with those obtained using multi-precision and the Rigorous Coupled Wave Analysis (RCWA).

<http://dx.doi.org/10.1364/ao.XX.XXXXXX>

1. INTRODUCTION

Introduced in 1980, the C method, or Chandezon method [1][2] [3], is a rigorous model for the diffraction of light by a grating. This method solves the propagation equation written in a coordinate system (u, v) such that the grating surface is a surface of constant v . In the (u, v) system, the propagation equation involves the non-linear profile function of the grating through its derivative. Taking into account the periodicity, this propagation equation is associated with a matrix operator called the Maxwellian, which is the electromagnetic wave equivalent of the Hamiltonian for matter waves. The incident and diffracted fields are expressed as a linear combination of Maxwellian eigenvectors. This method yields excellent results provided the height of the grating profile function is not large relative to its period. However, for a sinusoidal grating with a period of a few wavelengths, increasing the height encounters a numerical modeling limitation akin to a numerical wall that cannot be surpassed. This wall manifests as poor matrix conditioning when writing boundary conditions at the surface of the grating, rendering inversions impossible. Various methods have been developed to overcome these challenges, such as analytical regularization [4], or increasing the calculation precision, using a parametric coordinate system [5], or working with multi-precision [6] [7] [8]. Despite making the calculations more complex, none of these methods are satisfactory.

It is commonly believed that the wall is caused by accumulated rounding errors, but this is only partially true. The numerical difficulties are not solely related to the calculation method but rather to the phenomenon itself; it is a consequence of the non-linearity of the propagation equation concerning the geometry of the diffracting objects. A slight perturbation in the grating's shape leads to a significant variation in the solution, which is characteristic of non-linearity. A mathematical technique known as the resolution of stochastic differential equations (SDE) can be used to address this type of problem. With the SDE method, a deterministic solution is not sought, but rather a probabilistic or stochastic solution. It is straightforward to acquire a stochastic solution with the classical C method or CCM by introducing Brownian numerical noise onto the grating profile. This change yields the stochastic C method or SCM. With the SCM, a decisive result occurs: for sinusoidal gratings, the numerical problems are resolved. Whereas with the CCM, difficulties arise for sinusoidal gratings with a height-to-period ratio of $h/d \gtrsim 3$. With the SCM it is possible for the h/d ratio to exceed 50. What is most remarkable is that to achieve this improvement, it is unnecessary to overhaul the CCM calculation code. Simply adding a line or two of code that introduces noise generation suffices.

There are additional practical advantages to using the SCM method over the CCM. Summary statistics can be obtained by computing the confidence interval of a preset number of com-

puted results. Those summary statistics afford precision values which indicate how many significant figures should be considered for these results, as well as confidence intervals for obtaining results.

Obtaining results in a probabilistic form for diffraction problems can be seen as a natural approach. When calculating a grating's efficiency, what is calculated is not deterministic because it is the probability for an incident photon to emerge in a given diffraction order. What may seem to be deterministic in the classical formulation of diffraction is, in fact, probabilistic. This is the source of the computational difficulties since to increase the precision of the results in determining probabilities, the volume of calculations must increase much more rapidly.

Section 2 introduces the Maxwellian calculated from the propagation equation in the translation coordinate system (u, v) . Section 3 recalls how the Maxwellian eigenvectors are used to determine the waves diffracted by a grating. In Section 4, in the case of two very similar-shaped gratings, the effect of non-linearity is highlighted. In Section 5, the stochastic C method SCM is implemented in a few examples. Section 6 analyzes the precision achievable in a grating diffraction problem.

2. THE 2D PROPAGATION EQUATION

This study considers harmonic electromagnetic waves of frequency ν with angular frequency ω , and with a vacuum wavelength of $\lambda = c/\nu$, where c is the speed of light in vacuum, and $k = 2\pi/\lambda$ is the wave vector. The temporal dependence of the fields is given by $\partial/\partial t = i\omega$. The propagation occurs in homogeneous and isotropic media with a refractive index of n . The study is restricted to 2D problems for which $\partial/\partial z = 0$.

A. Propagation equation in Cartesian Coordinates

Maxwell's equation written in Cartesian coordinates shows that any component of the electromagnetic field, denoted by F , obeys the same scalar propagation equation, which is the Helmholtz equation:

$$\frac{\partial^2 F}{\partial x^2} + \frac{\partial^2 F}{\partial y^2} + n^2 k^2 F = 0. \quad (1)$$

There are two types of independent solutions denoted as **TE** polarization and **TM** polarization. Only three Cartesian components of the field are non-zero for either polarization state: E_z, H_x, H_y for **TE** polarization and H_z, E_x, E_y for **TM** polarization. Since the propagation equation is identical for both polarizations in a homogeneous medium, we denote by the same letter F the E_z and the H_z field components for the **TE** and **TM** polarizations, respectively. It is observed that during propagation, the electromagnetic wave behaves like a scalar wave. It is only when writing the boundary conditions at the grating profile's surface that the electromagnetic field's vectorial behavior becomes apparent. The eigensolutions of the Helmholtz equation are propagating or evanescent plane waves, which are expressed as:

$$F(x, y) = A(\alpha) e^{-ik\alpha x} e^{-ik\beta y} d\alpha \quad (2)$$

, where α is the propagation constant along Ox and β is the propagation constant along Oy . α and β satisfy the dispersion equation: $\alpha^2 + \beta^2 = n^2$. If the constant α is known, the determination for β is as follows:

$$\begin{cases} \beta^\pm = \pm \sqrt{n^2 - \alpha^2} & \text{if } \alpha^2 \leq n^2 \\ \beta^\pm = \mp i \sqrt{\alpha^2 - n^2} & \text{if } \alpha^2 > n^2 \end{cases} \quad (3)$$

For each polarization, there are two types of solutions:

- F^+ , composed of plane waves propagating in the direction of increasing y and evanescent waves attenuating in the direction of increasing y .
- F^- , composed of plane waves propagating in the direction of decreasing y and evanescent waves attenuating in the direction of decreasing y .

B. Propagation equation in translation coordinates

New coordinates

The 2D translation coordinate system (u, v) is defined from the 2D Cartesian system (x, y) by the following transformation:

$$\begin{cases} u = x \\ v = y - ha(x) \end{cases} \quad \text{and} \quad \begin{cases} x = u \\ y = v + ha(x) \end{cases} \quad (4)$$

The z coordinate does not come into play in 2D problems. The coordinate surfaces $v = \text{const}$ are invariant cylindrical surfaces along Oz with a section $y = ha(x) + \text{const}$, where $a(x)$ is the normalized profile function such that $0 \leq a(x) \leq 1$ and h is the amplitude. We define $\dot{a}(x) = ha'(x)$ where $a'(x) = da/dx$. After the change of variables in (1), the propagation equation satisfied by $F(u, v)$ in the (u, v) system is written as:

$$\frac{\partial^2 F}{\partial u^2} + n^2 k^2 F - \frac{\partial}{\partial u} \dot{a} \frac{\partial F}{\partial v} + \frac{\partial}{\partial v} \left((1 + \dot{a}^2) \frac{\partial F}{\partial v} - \dot{a} \frac{\partial F}{\partial u} \right) = 0. \quad (5)$$

This second-order propagation equation in v is nonlinear concerning \dot{a} . To solve it, we need to transform it into a system of two first-order equations in v . To do this, we introduce the following function $G(u, v)$:

$$ikG(u, v) = (1 + \dot{a}^2) \frac{\partial F}{\partial v} - \dot{a} \frac{\partial F}{\partial u}. \quad (6)$$

By setting $c = 1/(1 + \dot{a}^2)$, this yields a first-order equation in v :

$$\frac{\partial F}{\partial v} = \dot{a} c \frac{\partial F}{\partial u} + ikcG. \quad (7)$$

By introducing the expression of G (Eq. 6) into the propagation equation (Eq. 5), we obtain the second first-order equation, allowing us to write the following system of two first-order equations in v :

$$\begin{cases} \frac{\partial F}{\partial v} = \dot{a} c \frac{\partial F}{\partial u} + ikcG \\ \frac{\partial G}{\partial v} = \frac{i}{k} \left(n^2 k^2 + \frac{\partial}{\partial u} c \frac{\partial}{\partial u} \right) F + \frac{\partial}{\partial u} \dot{a} c G \end{cases} \quad (8)$$

Resolution of the propagation equation

We seek solutions of the system (8) such that: $\partial_v = -ikr$.

By setting $\partial/\partial u = \partial_u$, we obtain the following eigenvalue system:

$$r \begin{bmatrix} F \\ G \end{bmatrix} = \begin{bmatrix} ik^{-1} \dot{a} c \partial_u & -c \\ -n^2 - k^2 \partial_u c \partial_u & ik^{-1} \partial_u \dot{a} c \end{bmatrix} \begin{bmatrix} F \\ G \end{bmatrix}. \quad (9)$$

3. MAXWELLIAN

This can be written as:

$$r\Psi = \mathbf{M}\Psi, \quad (10)$$

where Ψ is an electromagnetic wave function, symbolically, this equation is of the same type as the Schrödinger equation in quantum mechanics, where the operator is the Hamiltonian; that's why we call \mathbf{M} the Maxwellian. The general solution to this equation is a linear combination of the eigensolutions ψ_n of \mathbf{M} .

A. The Maxwellian in periodic coordinates

We seek an expression of F in the Hilbert space of pseudo-periodic functions of v with period d , meaning periodic up to a phase factor. In this space, the continuous functional operators ∂_u and \hat{a} are represented by matrices.

Propagation matrix The periodicity with respect to v leads to associating the derivative with respect to u with a diagonal matrix $\partial_u \Rightarrow -ik\alpha$, where:

$$\alpha_{m,m} = \alpha_0 + m \frac{\lambda}{d}, \text{ and } \alpha_{m,n} = 0 \text{ if } m \neq n. \quad (11)$$

Normalized matrices associated with \hat{a} and \mathbf{c} $a(x)$ can be expanded as a Fourier series :

$$a(x) = \sum_{m=-\infty}^{+\infty} a_m e^{-i2\pi mx/d}, \quad (12)$$

where:

$$a_m = \frac{1}{d} \int_{x=0}^d a(x) e^{+i2\pi mx/d} dx. \quad (13)$$

The Fourier coefficients a_m of $a(x)$ are dimensionless. If $a(x)$ is differentiable, its derivative $a'(x)$ can be written as:

$$a'(x) = -i \frac{2\pi}{d} \sum_{m=-\infty}^{+\infty} m a_m e^{-i2\pi mx/d}. \quad (14)$$

The function $ha'(x)$, is associated with the dimensionless Toeplitz matrix $\hat{\mathbf{a}}$ whose coefficients are:

$$\hat{a}_{m,n} = -i \frac{2\pi h}{d} (m-n) a_{m-n}. \quad (15)$$

The function $c(x)$ is associated with the matrix \mathbf{c} such that:

$$\mathbf{c} = (\mathbf{I} + \hat{\mathbf{a}}\hat{\mathbf{a}})^{-1}. \quad (16)$$

B. The Maxwellian matrix

In the (u, v) system, in matrix form, the Maxwellian is written as:

$$r \begin{bmatrix} F \\ G \end{bmatrix} = \begin{bmatrix} \hat{\mathbf{a}}\mathbf{c}\alpha & -\mathbf{c} \\ -n^2 + \alpha\mathbf{c}\alpha & \alpha\hat{\mathbf{a}}\mathbf{c} \end{bmatrix} \begin{bmatrix} F \\ G \end{bmatrix}. \quad (17)$$

The set of functions F and G form an electromagnetic wave function Ψ with two components. To express vectors, we adopt Dirac's "bracket" notation, where "bras" are row vectors denoted as $\langle f|$ and "kets" are column vectors denoted as $|f\rangle$. The Hermitian product is a "bracket" $\langle f|g\rangle$. With these notations, the electromagnetic wave function is written as:

$$|\Psi\rangle = \begin{bmatrix} |F\rangle \\ |G\rangle \end{bmatrix}. \quad (18)$$

The eigenvalue equation is written as:

$$r|\Psi\rangle = \mathbf{M}|\Psi\rangle. \quad (19)$$

The Maxwellian eigenvalues are denoted as r_n and the eigenvectors as $|\psi_n\rangle$. Any solution $|\Psi\rangle$ of the wave equation can be written as a linear combination of the $|\psi_n\rangle$, i.e.:

$$|\Psi\rangle = \sum_{n=-\infty}^{+\infty} A_n |\psi_n\rangle. \quad (20)$$

The coefficients A_n are either the given data or the unknowns of the diffraction problem.

Maxwellian eigenvalues

To be able to search numerically eigenvectors of the Maxwellian, we need to limit the size of the matrices, α and $\hat{\mathbf{a}}$, to $2M+1$ rows and columns, retaining only M components in the Fourier space. We call this the M approximation. To numerically compute the Fourier coefficients a_m of $a(x)$, we need to use $2M$ samples of the profile $y_i = a(x_i)$. In the M approximation, the Maxwellian is a non-Hermitian square matrix of dimension $2(2M+1)$, which has $2(2M+1)$ eigenvalues r_n . For a lossless medium, the real eigenvalues represent the far field whereas the imaginary or complex eigenvalues represent the near field. Depending on the nature of the eigenvalues, we can categorize the eigenvectors into four sets of dimensions $2M+1$. The set of eigenvectors ψ_n forms a $2(2M+1)$ matrix, which is divided into 4 sub-matrices $\mathbf{F}^\pm, \mathbf{G}^\pm$ according to Table 1. With these notations, on the surface

Re(r)	Im(r)	F	G	Propagation
> 0	0	\mathbf{F}^+	\mathbf{G}^+	$v \nearrow$
< 0	0	\mathbf{F}^-	\mathbf{G}^-	$v \searrow$
\sim	< 0	\mathbf{F}^+	\mathbf{G}^+	$v \nearrow$
\sim	> 0	\mathbf{F}^-	\mathbf{G}^-	$v \searrow$

Table 1. Distribution of the eigensolutions of the Maxwellian

$v = 0$, the electromagnetic wave function is written as:

$$|\Psi\rangle = \begin{bmatrix} |F\rangle \\ |G\rangle \end{bmatrix} = \begin{bmatrix} \mathbf{F}^+ & \mathbf{F}^- \\ \mathbf{G}^+ & \mathbf{G}^- \end{bmatrix} \begin{bmatrix} |A^+\rangle \\ |A^-\rangle \end{bmatrix}. \quad (21)$$

Kets $|A^+\rangle$ and $|A^-\rangle$ represent the amplitudes of the eigensolutions.

Wave function continuity

At the surface Σ of the grating, the continuity of $|\Psi\rangle$ must be enforced for polarization **TE** and of $\sigma|\Psi\rangle$ for polarization **TM**, where σ is the following matrix:

$$\sigma = \begin{bmatrix} \mathbf{I} & \mathbf{0} \\ \mathbf{0} & \mathbf{I}/n^2 \end{bmatrix}. \quad (22)$$

Energy considerations

The Hermitian product $\langle \bar{F}_n | G_n \rangle$ where \bar{F} is the complex conjugate of F , represents the energy diffracted by the eigensolution $|\psi_n\rangle$ through one period of Σ . If the eigenvectors $|\psi_n\rangle$ are normalized with the Hermitian product $\langle \bar{F}_n | G_n \rangle$, then the probability \mathcal{P}_n that an incident photon is diffracted in direction n is given by $\mathcal{P}_n = A_n \bar{A}_n$.

4. APPLICATION TO DIFFRACTION BY GRATINGS

A. Diffraction by gratings

A surface relief grating (Fig. 1) consists of a cylindrical surface Σ separating two half-spaces Ω_1 and Ω_2 with different refractive indices. In the following, the medium Ω_1 is vacuum and Ω_2 is a medium with optical index n . Surface Σ is an invariant cylindrical surface along Oz with cross-section $y = ha(x)$. In the translation system, the grating surface is the surface with coordinate $v = 0$.

The grating is illuminated by a monochromatic plane wave with wavelength λ , incident angle θ_0 , and wave vector \vec{k} , where $k = \omega/c$ and c is the speed of light in vacuum.

The normalized component F of the incident field along Oz is given by:

$$F = e^{-ik \sin \theta_0 x} e^{-ik \cos \theta_0 y}. \quad (23)$$

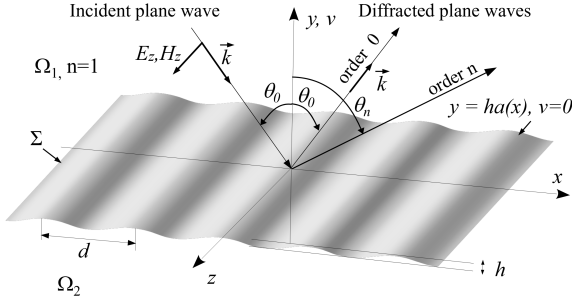


Fig. 1. Plane wave diffraction by a grating

Due to the periodicity of $a(x)$, in Cartesian Coordinates, the diffracted electromagnetic field can be expressed as a sum of plane waves and evanescent waves called the Rayleigh expansion. In Ω_1 , F is written as:

$$F = \sum_{n=-\infty}^{+\infty} A_n e^{-ik\alpha_n x} e^{-ik\beta_n y}, \quad (24)$$

with:

$$\alpha_n = \sin \theta_0 + n \frac{\lambda}{d} \text{ and } \beta_n^2 = 1 - \alpha_n^2. \quad (25)$$

Let U_d be the set of values of n such that $|\alpha_n| < 1$:

$$U_d = \left\{ n \in \mathbb{Z}, \left| \sin \theta_0 + n \frac{\lambda}{d} \right| < 1 \right\}. \quad (26)$$

If $n \in U_d$, then $\alpha_n = \sin \theta_n$, i.e., $\sin \theta_n = \sin \theta_0 + n \frac{\lambda}{d}$, which gives $\beta_n = \sqrt{1 - \sin^2 \theta_n} = \cos \theta_n$. The corresponding term in the Rayleigh expansion (24) is a plane wave with diffraction angle θ_n . If $n \notin U_d$, then $\beta_n = -i\sqrt{\alpha_n^2 - 1}$, corresponding to an evanescent wave attenuating in the y direction.

B. Resolution in the translation coordinates system

Solving the diffraction problem by the grating Σ consists of writing the continuity conditions of the wave function across Σ and determining the coefficients A_n of the Rayleigh expansion based on those of the incident wave.

The perfectly conducting grating

In this case, the resolution of the Maxwellian is only done in Ω_1 . For the TE polarization, F is zero on Σ , F_1^- represents the matrix of incident waves with amplitudes $|A_1^- \rangle$, and F_1^+ represents those of diffracted waves with amplitudes $|A_1^+ \rangle$. For the TM polarization, it is enough to replace F by G . The following linear system allows us to determine the amplitudes $|A^+ \rangle$ of the diffracted field based on the amplitudes $|A_1^- \rangle$ of the incident field, with:

$$S = [F^+]^{-1} F^- \text{ for TE, and } S = [G^+]^{-1} G^- \text{ for TM} \quad (27)$$

Remark If we interchange F_1^+ with F_1^- and G_1^+ with G_1^- we obtain the results for the opposite surface Σ^- with profile $-a(x)$.

Other gratings

Other gratings include pure dielectric gratings and gratings for which the optical index in Ω_2 is complex. In that case, one must also solve the Maxwellian in Ω_2 to determine the matrices of the eigenvectors F_2^+ , F_2^- , G_2^+ and G_2^- .

B.1. Polarization TE

At the surface Σ the wave function is known:

$$\begin{bmatrix} F_1^- & F_1^+ \\ G_1^- & G_1^+ \end{bmatrix} \begin{bmatrix} |A_1^- \rangle \\ |A_1^+ \rangle \end{bmatrix} = \begin{bmatrix} F_2^+ & F_2^- \\ G_2^+ & G_2^- \end{bmatrix} \begin{bmatrix} |A_2^+ \rangle \\ |A_2^- \rangle \end{bmatrix}, \quad (28)$$

where the ket $|A_p^\pm \rangle$, $p = 1, 2$ are the amplitude of the incident and diffracted waves at Σ . According to table 1, for the physical problem at hand, we have the following correspondence:

- $|A_1^- \rangle$ > amplitude of the incident wave in Ω_1 ,
- $|A_1^+ \rangle$ > unknown amplitudes of the reflected waves in Ω_1 ,
- $|A_2^- \rangle$ > unknown amplitudes of the transmitted waves in Ω_2 ,
- $|A_2^+ \rangle$ > amplitudes of the incident waves in Ω_2 which are assumed to be zero.

We are searching for the diffracted amplitudes $|A_1^+ \rangle$ and transmitted amplitudes $|A_2^- \rangle$ as functions of the incident amplitudes $|A_1^- \rangle$ and $|A_2^+ \rangle$, which leads to the following scattering matrix S :

$$\begin{bmatrix} |A_1^+ \rangle \\ |A_2^- \rangle \end{bmatrix} = \begin{bmatrix} S_{1,1} & S_{1,2} \\ S_{2,1} & S_{2,2} \end{bmatrix} \begin{bmatrix} |A_1^- \rangle \\ |A_2^+ \rangle \end{bmatrix}, \quad (29)$$

with:

$$S = \begin{bmatrix} F_1^+ & -F_2^- \\ G_1^+ & -G_2^- \end{bmatrix}^{-1} \begin{bmatrix} -F_1^- & F_2^+ \\ -G_1^- & G_2^+ \end{bmatrix}. \quad (30)$$

In practice, there is no incident wave in Ω_2 , so $|A_2^+ \rangle = 0$, which gives:

$$|A_1^+ \rangle = S_{1,1} |A_1^- \rangle \text{ and } |A_2^- \rangle = S_{2,1} |A_1^- \rangle. \quad (31)$$

B.2. TM Polarization

The calculation is practically identical to that of TE polarization, the only difference being that one must connect G/n^2 instead of G . The diffraction matrix S is expressed as:

$$S = \begin{bmatrix} F_1^+ & -F_2^- \\ G_1^+ & -G_2^-/n^2 \end{bmatrix}^{-1} \begin{bmatrix} -F_1^- & F_2^+ \\ -G_1^- & G_2^+/n^2 \end{bmatrix}. \quad (32)$$

As for TE polarization, if $|A_2^+ \rangle = 0$, we obtain:

$$|A_1^+ \rangle = S_{1,1} |A_1^- \rangle \text{ and } |A_2^- \rangle = S_{2,1} |A_1^- \rangle. \quad (33)$$

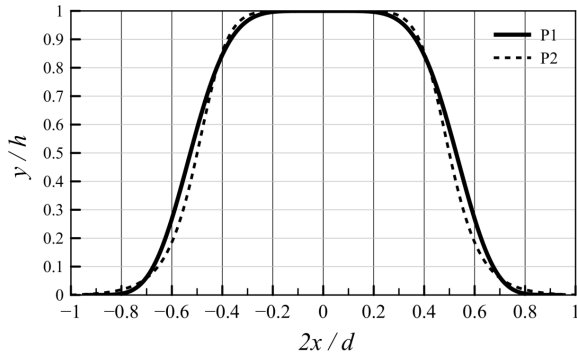


Fig. 2. Comparison of the shape of profiles P1 and P2.

5. SENSITIVITY OF DIFFRACTION TO THE GEOMETRY OF THE PROFILE

271
272

273 Mathematically, if the quantum aspect of the field is disregarded,
274 the C-method is a rigorous deterministic method. Theoretically,
275 with sufficient computational resources, it is possible to calculate
276 efficiencies with the C-method as precisely as desired, based on
277 the geometry of the grating. Computational implementations of
278 the original C-method have an envelope of parameters where
279 solutions can be successfully obtained. Ill-conditioned matrices
280 are most commonly encountered when the height of a grating
281 profile is large relative to the grating period. This is especially
282 evident in the case of sinusoidal gratings. The poor conditioning
283 could be interpreted as a defect of the C method; in reality, the
284 underlying reason is quite different.

285 In general, the poor conditioning of a linear system results
286 from the sensitivity of the solution to the problem's data. This
287 sensitivity is encountered in nonlinear differential systems, such
288 as diffraction by a grating. In this case, the grating geometry
289 intervenes non-linearly in the Maxwellian through the deriva-
290 tive $a'(x)$ of the profile. It is this non-linearity that causes the
291 computational difficulties.

Demonstrating sensitivity to geometry

292

293 The high sensitivity of diffraction to geometry can be highlighted
294 by comparing the results obtained with the C method for two
295 gratings with very similar shapes: P1 with profile $a_1(x) =$
296 $1 - (\sin^6 \pi x/2)^4$ and P2 with profile $a_2(x) = 1 / (1 + (2x)^8)$.
297 Grating P1 is the one considered by Xu and Li in [8]. Figure 2
298 shows how close to each other these two profiles are.

299 The non-linear behavior of the geometry is illustrated in Figs
300 3 and 4. Figure 3 shows the zeroth order efficiencies for
301 perfectly conducting gratings P1 and P2 when height h is varied
302 whereas Figure 4 shows the distribution of the eigenvalues r_n in
303 the complex plane. The chosen operating point is: $d = 1.25\mu\text{m}$,
304 $\lambda = 0.75\mu\text{m}$, $\theta_0 = 20^\circ$. It is observed that although the two
305 profiles are geometrically very similar, the results are dissimilar.
306 This is a consequence of the nonlinear behavior of geometry in
307 the Maxwellian which is the main cause of poor conditioning.

6. THE STOCHASTIC C METHOD

308

A. Stochastic aspect of diffraction

309

310 In classical numerical modeling, it is assumed that the param-
311 eters of the grating are known with absolute certainty. These
312 parameters include the Fourier spectrum of the derivative of
313 the profile $a'(x)$, the period d , and the refractive index n of the

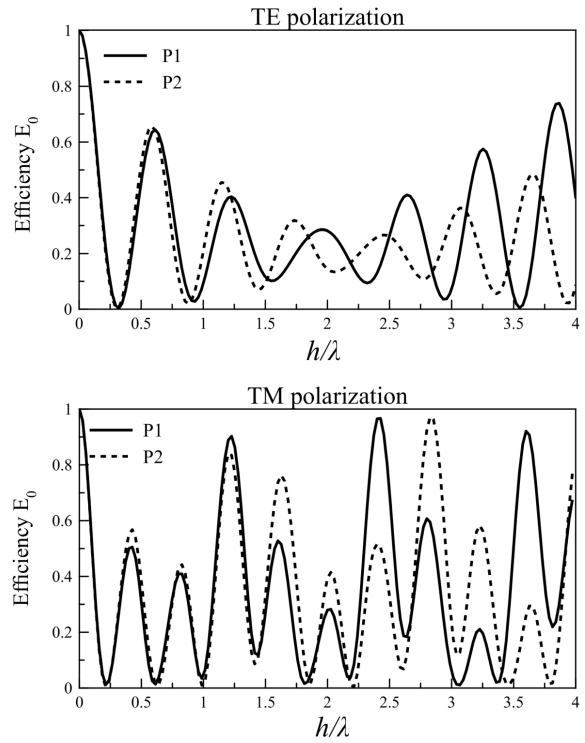


Fig. 3. zeroth order reflected efficiencies of both polarization states for perfectly conducting gratings with profiles P1 or P2 when height is varied

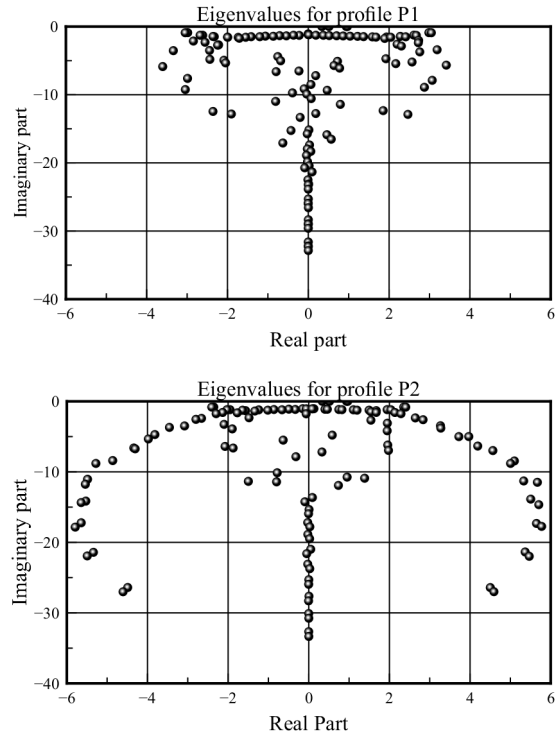


Fig. 4. Distribution of the computed eigenvalues for profiles P1 and P2

medium. In a linear problem, the assumption that the parameters are perfectly known poses no problem, which is not the case in a non-linear problem like diffraction. Stochastic resolution involves assuming that the data are affected by an irreducible uncertainty, which is numerically modeled as Brownian noise added to their theoretical values. The direct consequence is that modeling, which was perfectly deterministic, becomes probabilistic.

To overcome this numerical barrier, we have sought a solution to the difficulties attributable to the classic C-method by using stochastic differential equations [9], [10], [11]. Instead of seeking a rigorous, possibly inaccessible solution, a probabilistic solution that inherently contains uncertainty due to the stochastic nature of the equations is obtained.

B. Uncertainty on the shape of the grating

Once it is acknowledged that the profile is not deterministic but rather stochastic, instead of performing calculations for a profile $a(x)$, calculations are conducted for a random profile close to $a(x)$, such as $a(x) + \delta a(x)$, where $\delta a(x)$ is a random function. From a numerical perspective, this involves randomly perturbing the samples (x_i, y_i) describing $a(x)$. This perturbation is created using a random number generator with a normal distribution, which, after normalization, provides Brownian noise δ_i such that $-0.5 < \delta_i < 0.5$. In the numerical model, the set of samples $(x_i, y_i = a(x_i))$ is replaced by a new stochastic set $(x_i, y_i + \tau \delta_i)$, where τ is a perturbation parameter of the order 10^{-6} of the unit normalized profile. From an experimental standpoint in optics, the perturbation is typically so small that the perturbed profile appears identical to the unperturbed one.

Once this very small change is made in the numerical modeling, the numerical barrier disappears, allowing for the treatment of very deep gratings. In the case of sinusoidal gratings, heights of up to 100λ can sometimes be reached, albeit with a slight loss of precision.

The results obtained with the stochastic C-method approach are nondeterministic in that each program execution yields slightly different results. This presents the advantage, when using Monte Carlo methods, of determining a confidence interval for the efficiencies, avoiding the need to provide results with many non-significant decimal places.

C. Uncertainty on the period of the grating

The Maxwellian involves the nonlinear dependence of the diffraction directions matrix α on the grating period d . This indicates that, similar to $a(x)$, α can be affected by numerical noise. Numerical experiments show that, in the case of a sinusoidal grating, a very small noise on the order of 10^{-8} is also sufficient to eliminate poor conditioning.

D. Uncertainty on the optical index

In the modeling, the propagation medium is assumed to be perfectly homogeneous, with a known refractive index n that is constant throughout space. Similar to the approach with $a(x)$, we can introduce Brownian noise to the refractive index. The index is then represented by a diagonal matrix, with each term chosen randomly close to n . Like with $a(x)$ and α , this method also helps remove the numerical barrier.

E. Revisiting the C-method

The introduction of numerical noise in the data leads to the abandonment of classical rigorous solutions in favor of stochastic

solutions. However, it allows the elimination of the numerical barrier and greatly extends the application domain of the C method. This upgrade only involves very minor modifications to a few lines of the code.

In our case, we introduced noise on $a(x)$ because by varying the noise on the profile shape, it is easy to determine the uncertainty of the results based on the acceptable uncertainty in geometry, and vice versa. It is entirely possible, if deemed necessary, to introduce noise simultaneously on $a(x)$, α , and n . Any or all of these modifications to the C-method are possible to offer a stochastic C-method.

7. NUMERICAL STUDY OF SCM

A. Accuracy of results

From a quantum standpoint, the efficiency of a grating in the n^{th} order corresponds to the probability \mathcal{P}_n that an incident photon, illuminating the grating in the zeroth order, is diffracted in the n^{th} order. Maxwell's equations enable us to compute this probability. Experimentally, this probability corresponds to the ratio between the number N_q of photons diffracted in the n^{th} order and the total number N of incident photons, i.e., $\mathcal{P}_n = N_q/N$. Similar to the dice game analogy, the diffraction of an incident photon into the n^{th} order follows a binomial probability distribution. If we use N incident photons, the dispersion of estimates of \mathcal{P} around the exact value \mathcal{P}_n decreases as $1/\sqrt{N}$ as N increases. This relationship illustrates that, as demonstrated in Lifeng Li's article, calculating efficiencies with a precision of 10^{-36} would require 10^{72} incident photons, whereas Avogadro's number is only 6.02×10^{23} . Most of the time a precision of $\sim 10^{-5}$ should be sufficient to obtain a result that appears deterministic rather than probabilistic.

Analysis of precision on efficiencies

To verify the precision of the SCM, we compared our results for both dielectric and metallic sinusoidal gratings with those obtained by Tishchenko using multi-precision and the Rigorous Coupled Wave Analysis (RCWA) method. For simplicity, we only present the results for the zeroth reflected order E_0 .

Dielectric grating in TE polarization $\lambda = 0.6328\mu\text{m}$, $d = 1\mu\text{m}$, $h = 2\mu\text{m}$, refractive index $n = 2.5 - 0i$, $\theta_0 = 19.471221^\circ$

- Rayleigh multi-precision 20×64 bits, $M = 375$: $E_0 = 0.004703635612724$
- RCWA, $M = 64,1600$ slices: $E_0 = 0.004701051643882$
- SCM, $\tau = 10^{-5}$, $M = 170$: $E_0 = 0.004703 \pm 0.0000015$

Metallic grating in TM polarization $\lambda = 0.6328\mu\text{m}$, $d = 1\mu\text{m}$, $h = 1,6\mu\text{m}$, indice $n = 0 - 5i$, $\theta_0 = 19.471221^\circ$

- CCM, $M = 35$, zero-order efficiency: $E_0 = 0.8204481009$
- Rayleigh multi-precision 25×64 bits, $M = 405$: $E_0 = 0.820444416116999$
- SCM, $\tau = 10^{-5}$, $M = 170$: $E_0 = 0.82044 \pm 0.00001$

In these examples, we observe that the Stochastic C Method achieves a precision on the order of 10^{-5} , with results in perfect agreement with those obtained by Tishchenko [6] [7]. This precision appears to be what is achievable with the SCM, and require knowledge of the grating profile with an accuracy on the order of 0.01 nanometers. This accuracy is comparable to

the size of atomic radii. With very precise adjustments of the parameters τ and M , and calculations in multi-precision, it is certainly possible, if necessary, to achieve higher precision.

B. Deep sinusoidal grating

Despite that the eigenvalues may be calculated with very high precision using the C-method, sinusoidal profiles exhibit poor conditioning when the height h increases. In the following, the calculations were performed using the Scilab software, which handles poorly conditioned matrices less effectively than Matlab. Therefore, the results may differ slightly between Scilab and Matlab.

With Scilab, for a given height, if the dimension $4M + 2$ of the Maxwellian is too large, poor conditioning appears even for very shallow gratings. Introducing numerical noise eliminates this problem; increasing M no longer leads to poor conditioning. Table (2) shows results for a silver sinusoidal grating up to a height-to-period ratio of 72.

The experimental parameters are the following: $\lambda = 0.75\mu\text{m}$, $d = 1\mu\text{m}$, $\theta_0 = 20^\circ$, complex optical index of silver [12] $n = 0.031165 - 5.1949i$, $\tau = 1/100000$.

h/d	M	E_0^{TE}	E_{-1}^{TE}	E_0^{TM}	E_{-1}^{TM}
1	11	0.3143	0.6758	0.1810	0.7924
3	33	0.5311	0.4394	0.6127	0.3243
6	60	0.1500	0.7961	0.0560	0.8278
12	90	0.8048	0.0873	0.7720	0.0033
24	120	0.2603	0.5320	0.4105	0.2205
48	240	0.0051	0.6662	0.1379	0.1120
72	320	0.3893	0.1122	0.1274	0.1203

Table 2. Efficiencies as a function of height for a sinusoidal grating, the uncertainty in the results is less than 10^{-4} .

In this table, we can see that the numerical barrier with the original C-method, which is around $h/d = 4$, has disappeared. It is easy to determine the number of significant digits provided by the code by performing multiple calculations and obtaining uncertainties in the calculated values. The results in this experiment have at least 4 significant digits over a very wide range of heights.

8. CONCLUSION

By employing the mathematical methods of stochastic differential equations, we have developed the SCM, which significantly expands the applicability of the CCM. This improvement only entails very minor modifications to the calculation's code. The difference between the CCM and the SCM is that while the CCM results are deterministic, the SCM results are probabilistic. Over a wide range of heights, efficiencies are calculated with 4 or 5 significant figures; using a Monte Carlo method, it is possible to determine the uncertainty in the results. Ultimately, the SCM opens up new horizons for the C method, which, with the SCM, is no longer limited by height. In conclusion, for smooth profiles, current modeling based on the CCM should be updated by transitioning to the SCM, which is straightforward from a programming standpoint.

For the moment, SCM has shown its effectiveness for smooth profiles. On the other hand, the parameterization of piecewise linear profiles, with discontinuous derivatives, combined with the adaptive spatial resolution technique makes it possible to treat trapezoidal profiles with quasi-vertical slopes. It is clear that a complete parametric study would be necessary to have a precise understanding of the SCM—a study that has not yet been conducted.

ANNEX

This annex shows that the G function introduced for solving the scalar propagating wave equation in translation coordinates is proportional to the tangential field component E_u and H_u for TM and TE polarizations, respectively.

Tangential components and the G function.

The tangential components to Σ are, for TE polarization: $E_z = F$ and H_u , and for TM polarization: $H_z = F$ and E_u , where E_u and H_u are the covariant components of \vec{E} and \vec{H} in the translation coordinates.

Coordinate Transformation from Cartesian to Covariant

In the (u, v) coordinate system, the covariant component V_u of a covariant vector $\vec{V}(x, y)$ like \vec{E} or \vec{H} is calculated from the Cartesian components V_x and V_y using the following relation:

$$V_u = \frac{\partial x}{\partial u} V_x + \frac{\partial y}{\partial u} V_y \Rightarrow V_u = V_x + \dot{a} V_y. \quad (34)$$

TE Polarization

The only non-zero Cartesian components of the fields are $E_z = F$, H_x , and H_y . Maxwell's equations written in the Cartesian system (x, y) lead to the following expressions for H_x and H_y in terms of F :

$$\begin{aligned} H_x &= i \frac{Z_0}{k} \frac{\partial F}{\partial y} & \Rightarrow H_x &= i \frac{Z_0}{k} \frac{\partial F}{\partial v} \\ H_y &= -i \frac{Z_0}{k} \frac{\partial F}{\partial x} & \Rightarrow H_y &= -i \frac{Z_0}{k} \left(\frac{\partial F}{\partial u} - \dot{a} \frac{\partial F}{\partial v} \right) \end{aligned} \quad (35)$$

, where $Z_0 = \sqrt{\mu_0/\epsilon_0}$. This leads to the following expression for H_u in terms of F :

$$H_u = i \frac{Z_0}{k} \left((1 + \dot{a}^2) \frac{\partial F}{\partial v} - \dot{a} \frac{\partial F}{\partial u} \right). \quad (36)$$

TM Polarization

The only non-zero components of the fields are $H_z = F$, E_x , and E_y . Maxwell's equations lead to the expressions for E_x and E_y in terms of F as follows:

$$\begin{aligned} E_x &= -i \frac{1}{n^2 k Z_0} \frac{\partial F_z}{\partial y} & \Rightarrow E_x &= -\frac{i}{n^2 k Z_0} \frac{\partial F}{\partial v} \\ E_y &= i \frac{1}{n^2 k Z_0} \frac{\partial F_z}{\partial x} & \Rightarrow E_y &= \frac{i}{n^2 k Z_0} \left(\frac{\partial F}{\partial u} - \dot{a} \frac{\partial F}{\partial v} \right) \end{aligned} \quad (37)$$

This leads to the following expression for E_u in terms of F :

$$E_u = -i \frac{1}{n^2 k Z_0} \left((1 + \dot{a}^2) \frac{\partial F}{\partial v} - \dot{a} \frac{\partial F}{\partial u} \right) \quad (38)$$

502 **Continuity of the tangential components at Σ** 503 Let's consider the function G defined as follows:

$$ikG = (1 + \dot{a}^2) \frac{\partial F}{\partial v} - \dot{a} \frac{\partial F}{\partial u}. \quad (39)$$

504 For both polarizations, G is proportional to the tangential component of the field H_u in TE polarization and E_u in TM polarization. When passing through the cylindrical surface Σ with profile $y = a(x)$ separating two media with different indices, continuity of E_u and H_u must be enforced. This implies the following continuity rule for F and G :

- 510 • TE polarization : F and G are continuous
- 511 • TM polarization: F and G/n^2 are continuous

512 **Funding.** This research received no external funding.513 **Acknowledgments.** The authors thank Olivier Parriaux and Casey Kneale for their insightful comments.515 **Disclosures.** The authors declare no conflicts of interest.516 **Data Availability Statement.** Data sharing does not apply to this article.518 **REFERENCES**

- 519 1. J. Chandezon, "Les équations de Maxwell sous forme covariante, application à l'étude dans les guides périodiques et à la diffraction par les réseaux," Theses, Université de Clermont-Ferrand II (1979).
- 520 2. J. Chandezon, G. Raoult, and D. Maystre, "A new theoretical method for diffraction gratings and its numerical application," *J. Opt.* **11**, 235 (1980).
- 521 3. J. Chandezon, M. T. Dupuis, G. Cornet, and D. Maystre, "Multicoated gratings: a differential formalism applicable in the entire optical region," *J. Opt. Soc. Am.* **72**, 839–846 (1982).
- 522 4. J. Chandezon, A. Y. Poyedinchuk, Y. A. Tuchkin, and N. Yashina, "Mathematical modeling of electromagnetic wave scattering by wavy periodic boundary between two media," *Prog. In Electromagn. Res.* **38**, 130–143 (2002).
- 523 5. X. Xu and L. Li, "Simple parameterized coordinate transformation method for deep- and smooth-profile gratings," *Opt. Lett.* **39**, 6644–6647 (2014).
- 524 6. A. V. Tishchenko, "Numerical demonstration of the validity of the rayleigh hypothesis," *Opt. Express* **17**, 17102–17117 (2009).
- 525 7. A. V. Tishchenko, "Rayleigh was right: Electromagnetic fields and corrugated interfaces," *Opt. Photon. News* **21**, 50–54 (2010).
- 526 8. X. Xu and L. Li, "Numerical stability of the c method and a perturbative preconditioning technique to improve convergence," *J. Opt. Soc. Am. A* **34**, 881–891 (2017).
- 527 9. S. Biswas and N. Ahmed, "Stabilization of systems governed by the wave equation in the presence of distributed white noise," *IEEE Trans. on Autom. Control.* **30**, 1043–1045 (1985).
- 528 10. R. C. Dalang, *The Stochastic Wave Equation* (Springer Berlin Heidelberg, Berlin, Heidelberg, 2009), pp. 39–71.
- 529 11. C. J. Roussel, A. Coatanhay, and A. Baussard, "Stochastic differential equations for the electromagnetic field scattered by the sea surface for remote sensing applications," in *40th Conference on stochastic processes and their applications (SPA)*, (University of Gothenburg and Chalmers University of Technology, Gothenburg, Sweden, 2018).
- 530 12. P. B. Johnson and R. W. Christy, "Optical constants of the noble metals," *Phys. Rev. B* **6**, 4370–4379 (1972).
- 531
- 532
- 533
- 534
- 535
- 536
- 537
- 538
- 539
- 540
- 541
- 542
- 543
- 544
- 545
- 546
- 547
- 548
- 549
- 550
- 551
- 552
- 553